**ORIGINAL PAPER**

# Synthesis and gas permeation of polynorbornene by dinuclear α−diimine Ni-based catalysts: Experimental and quantum chemistry modeling

Seyed Emadodin Shakeri[1] · Seyed Mohammad Mahdi Mortazavi[1] · Saeid Ahmadjo[1] · Gholam Hossein Zohuri[2]

## Abstract

In this work, polynorbornene (PNB) was synthesized via dual-core catalyst successfully and applied in the gas membrane applications. The microstructure and physical properties of resultant PNB were evaluated precisely. FESEM images showed that PNB membrane had a dense and porous microstructure. XRD results indicated that polynorbornene had two sharp peaks at 2θ nearly 10° and 20°. The results of DSC analysis exhibited that with the design of the new synthetic system, the $T_g$ reduced, though both molecular weight, and film-ability of polymer were improved significantly. A molecular weight of over $9 \times 10^5$ g/mol was obtained for PNB. The permeability values against $CO_2$ and $CH_4$ were 63.7 and 5.2 (Barrer), respectively, which were comparable with those of reported previously. Additionally, the obtained selectivity was 12.2. DFT-D simulation results showed that $O_2$ molecules have more tendencies to $C_7H_{12}$ than that of other gas molecules and better capability to adsorb onto $C_7H_{12}$.

**Keywords** Polynorbornene · Dual-core catalyst · Glass transition temperature · Gas permeability · Membrane

## Introduction

Norbornene and its derivatives are used in a wide variety of applications such as light-resistant materials, optical applications, electrical insulation, adhesives and rubbers [1–3]. These materials can be synthesized in two different ways, based on the desired properties in the final application [4, 5]. If the ring opening polymerization pathway is used, we will have rubber polynorbornene with unsaturated structures in the main chain. By contrast, in catalytic polymerization, we will have polynorbornene with the main chain structure of saturation that leads to the formation of both rigid mechanical properties along with high glass transition temperature ($T_g$) [6, 7]. These features endow polynorbornene as a fascinating candidate for gas separations applications. In this line, polynorbornene (PNB) synthesized by vinyl-addition (VA)

polymerization is a well-known candidate for this purpose [8–10].

Nevertheless, this kind of PNB has distinguished properties compared to conventional counterparts, synthesized by ring-opening metathesis polymerization, such as rigidity, bicyclic core of the norbornyl ring and the absence of any residual alkenes within the polymer backbone. These features give rise to the improvement of chemical stability in severe conditions like high thermal stability ˃400 °C, proper resistance against plasticization, resistance versus aging phenomena, promoting thermal transition temperatures, and the rise of free volume fraction in the solid-state polymer [11–14].

These outstanding properties are required for membrane-based applications that are faced with severe situations and huge amount of gas, for instance $CO_2$ separation from coal-fired power plants during post-combustion process [15], ion exchange membranes and fuel cell [16], $CO_2$ separation from natural gas, reverse osmosis process in the case of sea water desalination and separation of light hydrocarbons from natural petroleum gas [17–20].

Although great progress has been made in improving the properties of gas separation membranes in the last decade, there are still a number of weaknesses. These weaknesses

✉ Saeid Ahmadjo
  s.ahmadjo@ippi.ac.ir

1  Department of Engineering, Iran Polymer and Petrochemical Institute (IPPI), P.O. Box 14965/115, Tehran, Iran

2  Department of Chemistry, Faculty of Science, Ferdowsi University of Mashhad, P.O. Box 91775, Mashhad, Iran

have been mainly reported in the case of film-ability, brittleness of the prepared films and inferior elongation at break of samples [12, 21, 22].

According to literature survey, based on the published results, in most cases, polynorbornene and its derivatives synthesized by catalytic method (addition polymerization) possessed a higher permeability than polymers synthesized by ring opening method [12, 22, 23].

Some studies have also suggested that the catalytic system, besides increasing the molecular weight along with enhancing the physical and mechanical properties, will bring about a narrower molecular weight distribution compared to ring opening polymerization method [24]. In the case of catalytic systems, some studies have revealed that the active complex between nickel metal and the MAO co-catalyst is more stable than that of metal complexes such as palladium and titanium; hence can lead to higher molecular weight polymers [11, 25].

Recently, many studies have focused on the diimine nickel catalyst for the synthesis of aromatic and aliphatic olefinic monomers. All of the studies confirmed that these catalysts enhanced the catalyst properties including stability and activity in the comparison to the non-metallocene catalysts. It is worth mentioning that Peng and Chen [26] used diimine nickel catalyst for the polymerization and copolymerization processes of ethylene and some other aliphatic monomers. Moreover, these catalysts were successfully used for the synthesis of functional norbornene monomers in the studies of Wang et al. [27, 28].

Other researchers believe that the polymer microstructure is affected by the polymerization conditions and therefore different microstructures can be obtained by changing the reaction temperature, the type of solvent and the type of catalyst and co-catalyst [29, 30]. Zhao et al. have reported the preparation of a rigid random copolymer structure via nickel based catalyst in which the rotation around chain is difficult due to the spatial barrier made by the presence of the ring in the main chain [11]. In another study, nickel-catalyzed polynorbornene was introduced with an atactic structure in terms of ring placement in the chain structure.

Our studies showed that in the synthesis of this polymer, many research groups were encountered in several problems such as polymer insolubility, low molecular weight, and the lack of film formation due to the membrane fragility [31–33].

Regarding this fact, a dual-core catalyst was applied in this research so as to improve the physical–mechanical properties, film-ability of polynorbornene homopolymer as well as application in gas separation.

In spite of significant studies that have been carried out in the synthesis of polynorbornene and its derivatives for utilization in the membrane industry, the effect of dual-core catalysts on the properties of the synthesized polymer in the application of gaseous membranes has not been investigated. Therefore, the present research aims to examine this issue.

In our previous work, the synthesis of linear polyolefins and relevant copolymers was reported for nickel-based dual-core catalysts, and consequently acceptable results were obtained for increasing molecular weight and final polymer properties [34–36]. The results of our previous study [37] showed the dinuclear α–diimine Ni-based catalysts was more active in comparison to mononuclear α–diimine for polynorbornene synthesis. So, the dinuclear α–diimine was used for the synthesis of polynorbornene. In this line, this new generation of catalyst is utilized in the case of polynorbornene homopolymer to tackle its drawbacks and improve gas separation properties. Besides, the density functional theory simulation (DFT) was performed to better exploit the adsorption of gas molecules via polynorbornene.

## Simulation details

In order to evaluate the interaction mechanism between synthesized polymer and studied molecules, density functional theory (DFT) was used to gain more insights about the diffusivity of all gases into polynorbornene. All simulations were performed using the DMOL3 code of Materials Studio software by the Perdew-Burke-Ernzerhof (PBE) function at GGA level of theory. The electronic basis set used in this study was a double numerical plus polarization (DNP) set, which is the same as 6-31G** in Gaussian [38, 39]. In order to save time and cost in the simulation process, simplified models as the initial structure in DFT calculations must be considered. In this regard, a monomer of norbornene with a chemical formula $C_7H_{12}$ was regarded for modeling of polymer. The adsorption energy of each cluster ($E_{ads}$) was determined via following formula:

$$E_{ads} = E_{complex} - E_{gas\ molecule} - E_{C7H12} \qquad (1)$$

Where $E_{complex}$, $E_{gas\ molecule}$, $E_{C7H12}$ are the energy of the complex (gas molecule/monomer), gas molecule, and monomer, respectively, after geometry optimization. It has been reported that the interaction of gas molecules with norbornene monomer can be explained at the electronic level. Frontier molecular orbitals including HOMO and LUMO along with their relevant energies can be applied for evaluating the interaction process quantitatively. Consequently, the band gap of each isolated structure could be determined via HOMO ($E_H$) and LUMO ($E_L$) energies through the next formula:

$$\Delta E_{L-H} = E_L - E_H \qquad (2)$$

According to the Eq. (2), one can predict the reactivity, stability, and the conductance of each molecule, or
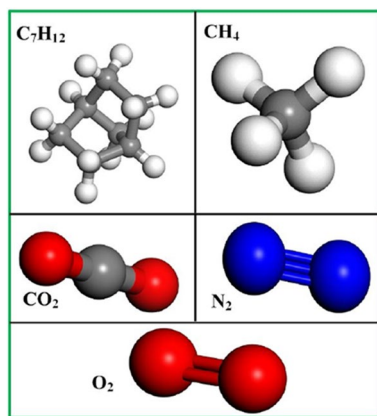
**Fig. 1** Geometry optimized molecules via DFT at GGA/PBE level of theory

cluster. Figure 1 shows the optimized structures of defined molecules.

# Experimental

## Materials

All the manipulations of air/water-sensitive compounds were conducted under $Ar/N_2$ atmosphere using the standard Schlenk technique. All the solvents were purified prior to use. Toluene was purchased from the Mojallaly Co. (99.9%) was purified over sodium wire/benzophenone, and used as polymerization media. Dichloromethane (96%, Sigma-Aldrich Chemicals, Germany) as solvents were purified over calcium hydride powder and distilled prior to use in the synthesis of complex and ligand. Chlorobenzene was purchased from Merck Chemical Co. Norbornene monomer and modified methylaluminoxane (MMAO, 7% in toluene) were supplied by Sigma Aldrich Chemicals (Steinheim, Germany).

## Ligands and complexes synthesis

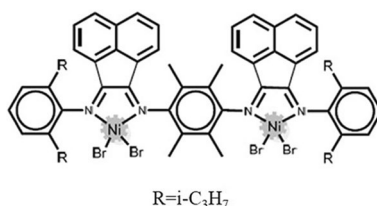The ligands and corresponding complexes were synthesized and fully described in our recent report [37] (Fig. 2).



R=i-$C_3H_7$

**Fig. 2** Structure of dinuclear α–diimine Ni-based catalysts

## Polymerization procedure

The synthesis approach of polynorbornene was performed based on our recently published paper [37]. The norbornene polymerization was carried out in a flask under Schlenk system. 7.52 g of norbornene, 16 ml toluene and MMAO 0.7% W/W solution in toluene were added in to the flask. Polymerization was started by adding catalyst in 2 ml dichloromethane. Reaction mixture was stirred at desired temperature for the required time. Reaction was quenched by adding acidified methanol. The precipitated polymer was filtered, washed with methanol for several times and then, dried in vacuum oven at 80 °C for 24 h.

## Film formation

The preparations of films were obtained via casting of 5% of polymer solution (by weight) in trichlorobenzene. To begin with, 1 g polymer was dissolved in 30 ml of trichlorobenzene and was allowed to stir for 4 days before obtaining a clear solution. Afterwards, the resultant solution was poured into a 5 cm diameter petri dish to form a membrane. The petri dish was covered with an aluminum foil and transferred under the hood for 12 h and then transferred to a vacuum oven at 80 °C to increase the solvent separation rate. After 5 days, the dried membranes were placed in a water tank for 3 h and then separated from the petri dish and used for permeability testing. The thickness of the prepared films was 20–80 μm.

## Characterization

The polymer molecular weight distribution (MWD) were determined with a high temperature gel permeation chromatography (GPC), run at $145^0C$ under a flow rate of 1,2,4-trichlorobenzene of 1 mL $min^{-1}$. The GPC was equipped with three detectors in series (infrared, light scattering, and differential viscometer) and calibrated with polystyrene narrow standards. The X-ray diffraction patterns were collected in transmission mode on a STOE Stadi P high-throughput powder diffraction apparatus equipped with a CuKα X-ray tube ($\lambda = 1.5418$ Å) and an image plate detector.

The morphological structure of both the surface and cross-section of the membranes was investigated by the field emission scanning electron microscope (FE-SEM, MIRA3 TESCAN, Czech Republic) operating at 10 kV acceleration voltage. Previously, the cross-section of the samples was prepared by fracturing in liquid nitrogen. The membrane surface and fractured surfaces were sputter-coated by a thin gold layer using a sputter coater (Q150R S, Quorum, England) during 60 s under 20 mA.

The permeability was studied by single-gas permeation using a constant-volume/variable-pressure apparatus. The

**Table 1** The properties of synthesized polymer compared to literature

| Polymer | catalyst | Al/Ni | $M_n$(kg/mol) | $M_w$(kg/mol) | PDI | Yield (%) | Ref |
|---|---|---|---|---|---|---|---|
| APN | Nibr$_2$[2,6-diisopropyl-C$_6$H$_2$-N=C-(C$_{10}$H$_6$)-C=N-C$_6$H$_4$-N=C-(C$_{10}$H$_6$)-C=N-2,6-diisopropyl-C$_6$H$_2$]/MAO | 1000 | 467 | 902 | 1.9 | 88 | **This work** |
| APN | Ni(C$_6$F$_5$)$_2$(SbPh$_3$)$_2$/MAO | 1000 | 84 | 277 | 3.3 | 58 | [37] |
| APN | Ni(acac)$_2$/MAO | 1000 | 388 | 730 | 1.9 | 72 | [11] |
| APN | Ni(Nph)$_2$/MAO | 1000 | 100 | 406 | 4.06 | 67 | [19] |
| APN | [Ni(methallyl)Cl]$_2$/MAO | 1000 | 142 | 366 | 2.58 | 83 | [19] |
| APN | [Pd(allyl)Cl]$_2$/MAO | 1000 | 285 | 661 | 2.32 | 82 | [19] |
| APN | Ni(C$_6$F$_5$)$_2$(SbPh$_3$)$_2$/AgSbF$_6$ | 2100 | 145 | 378 | 2.61 | 87 | [19] |

permeation cell was maintained at $28 \pm 2\ ^0$C. The feed pressure was $1 \pm 0.05$ atm, on the permeate side of the film, the gas pressure was less than 10 Torr and considered negligible.

The membrane thickness was measured by a Mitutoyo Disk micrometer (369–511-30, $\pm 4$ μm).

# Result and discussion

The prepared films firstly characterized with different methods and secondly permeability of film tested for $CO_2$, $CH_4$, $N_2$, $O_2$ gases and compared with other researches in literatures and finally DFT-D simulation used for investigation of the adsorption of gas molecules via polynorbornene film.

## Polymer characterization

Although the density of polynorbornene has been reported to be less than 1 g/cm$^3$, some researchers believe that the higher density leads to the higher permeability [21], which can be more significant in the case of polynorbornene synthesized by the dual-core catalyst. As a result, a density of nearly 1gr/cm$^3$ was obtained in this study.
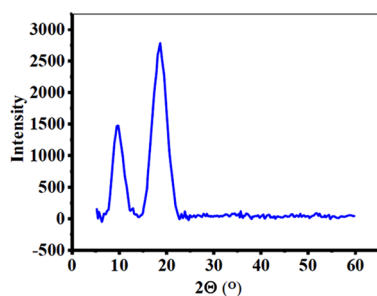
## Molecular weight

As shown in Table 1, the use of dual-core catalysts allows the synthesis of polynorbornene with a molecular weight of over $9 \times 10^5$ g/mol that is soluble in such solvents such as chlorobenzene (trichlorobenzene) family and the possibility of dissolution; hence the chance of membrane preparation by casting method was enhanced. However, this polymer is still brittle compared to conventional polymers and needs further work to improve film-formation ability properties.

As shown in Table 1, synthesized polynorbornene using a nickel-based dual-core catalyst associated with a methylaluminoxane cocatalyst had higher molecular weight and a narrow molecular weight distribution compared to similar studies reported by others.

## X-ray diffraction pattern

The XRD diffraction pattern of synthesized polynorbornene is illustrated in Fig. 3. Polynorbornene possesses two broad peaks in the X-ray diffractometer plot, confirming the completely amorphous nature of this polymer. The peak observed at higher 2θ (20°) is related to intra segmental interactions and the peak observed at lower 2θ (10°) is ascribed to the inter segmental interactions. The crystallinity outcomes are summarized in Table 2.



**Fig. 3** XRD pattern of polynorbornene

**Table 2** Crystalline properties of synthesized polynorbornene compared to reported data in the literature

| Polynorbornene | 2θ [°] | | Ref |
|---|---|---|---|
| | Low Angle | High Angle | |
| APN | 10 | 18.5 | [11] |
| APN | 10 | 18.8 | [37] |
| APN (R:-CH$_3$) | 9.5 | 18.2 | [23] |
| APN | 9.5 | 18.5 | This work |

The results are in agreement with those of previous reports [12, 21, 40] and confirm that, despite the significant increment in molecular weight, the possibility of crystal formation increased. However, the circular structures in the main chain are considered as a serious obstacle to the formation of crystalline structure in the polynorbornene family.

Based on XRD results, it can be concluded that small decrement in the diffraction angle further confirmed the positive influence of catalyst on the microstructure of polynorbornene. Besides, this decrease can be led to increasing of free volume and consequently better permeability.

## Thermal analysis

Overall, there is no obvious relation between $T_g$ and gas permeability properties. At temperatures below $T_g$, the main factor affecting the permeability properties is the free volume of polymer, which refers to its structure [22]. Note that $T_g$ can be a sign of chain stiffness, and increases over the increasing of chain stiffness [29].

Nevertheless, some researchers have indicated that the permeability properties enhance upon improving of chain stiffness [21]. They believed that with increasing chain stiffness, the final density of the polymer increases and the increase in density improves the performance of permeability. Also, with increasing the chain stiffness, although the number of pores inside the polymer decreases, the size of this cavity increases. In other words, due to the difficulty of moving and rotating the chain, changing the size of the pores is not possible. Consequently, the size of pores do not change during the function of the prepared membrane [23, 26].

The results of DSC analysis showed that with the design of the new synthetic system, the $T_g$ reduced but both molecular weight, and film-ability of polymer were improved significantly. Also the result of TGA test had been showed that the thermal stability of polynorbornene improved [37].

## Field emission scanning electron microscopy (FESEM)

FESEM images of synthesized polynorbornene are illustrated in Fig. 4. As can be seen, a dense and porous microstructure is evident from FESEM micrographs.

This is due to the type of solvent used in the polymer film forming process. In fact, due to the high evaporation temperature of trichlorobenzene, longer time is required for the solvent evaporation process from the polymer structure. This is favorable for creating numerous pores within polymer film during slow removal of solvent. Additionally, the porous structure of film is desirable for permeability application. This behavior has been previously confirmed in the case of synthesized polymer in the presence nickel based catalyst compared to that of synthesized in the existence of palladium. In fact, the resultant morphology of synthesized polymer via nickel catalyst had smoother surface as well as a lot of pores [19].

**Fig. 4** FESEM micrographs of **A** membrane surface and **B** cryo-fractured surface at different magnifications of **A-1** 2, **A-2** 1 μm, **B-1** 10 μm and **B-2** 1 μm
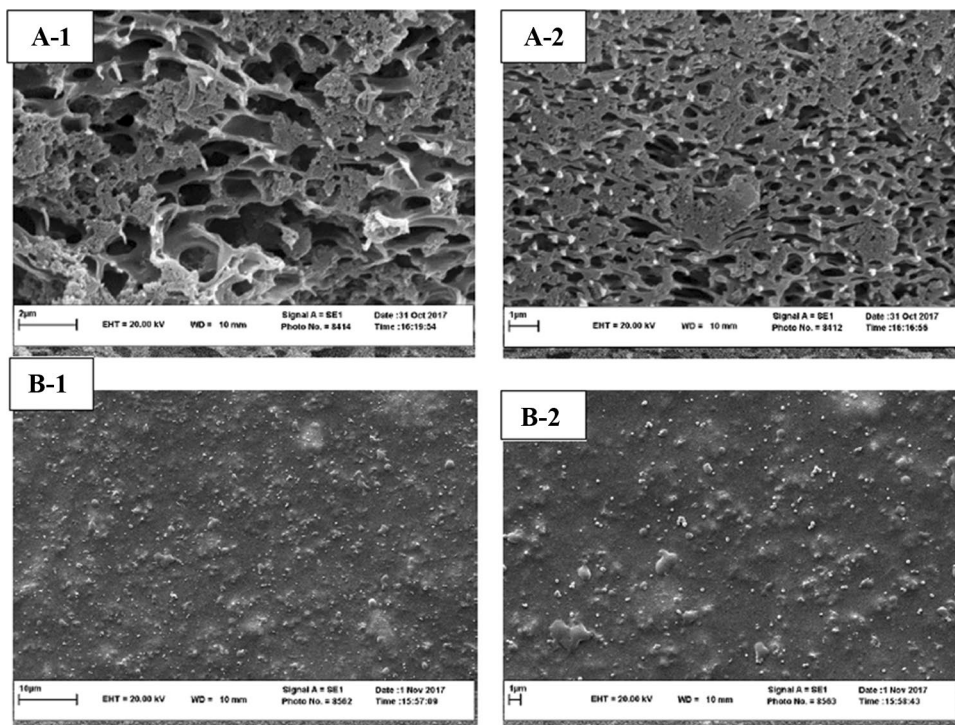
## Permeability results

The free volume within the polymer structure plays the vital role in the permeability properties of glass polymers, but it should be noted that the family of polynorbornene and its derivatives do not have a high free volume and the relative free volume of this family is mainly reported between 9 and 16%. There is not much difference between the relative free volume between polymers synthesized by catalytic and ring-opening methods [13.17].

It seems that one of the reasons for the low free volume of the polynorbornene family is the lack of side chain in their structure and also the high stiffness of the polymer chain which has low mobility, and thus affects the free volume. This problem is also manifested in the density so that with increasing the stiffness of the chain, the density of the polymer increases and consequently the free volume of the polymer decrease [23].

Most of the researches on the membrane properties of polynorbornene and its derivatives have been stated that the permeability and selectivity of polynorbornene synthesized using the catalytic system were substantially more than those of polymer synthesized by ring opening method [12, 38, 39].

Sundell et al., have deduced that the effect of $T_g$ reduction in the synthesized polynorbornene can be related to the decrease of kinetic resistance against the gas permeability. Therefore, it can be concluded that reducing the $T_g$ of the synthesized polynorbornene in the present work from about 300 $^0$C to around 240 $^0$C, had a positive effect on the improvement of the permeability properties compared to similar studies. In fact, lowering the $T_g$ leads to greater mobility of the chains and consequently enhancing gas permeability properties through the polymer [24].

As shown in Table 3, using dual-core catalysts, the solubility and film ability properties of polynorbornene membranes was improved. Moreover, a slight change in the free volume structure along with increasing the distance between the chains was observed in which membrane has a quasi-dense structure on the one hand and a porous structure on the other, the rate of membrane permeability is close to that of methyl group structures in the lateral branch. As we know according to Robson trade off line for gas separation membranes it is expected that as the permeability of membrane increases, Its selectivity decreases but As seen, the selectivity of the membrane was not changed much compared to similar samples in the literature [25, 40].

Aforementioned parameters may yield the improvement of permeability [4, 23]. However, in this study, we partially reduced this weakness in the polynorborn membrane with no side-chain by forming a membrane with variable porosity across the membrane.

## The permeability values against $CO_2$ and $CH_4$

The research groups that have investigated the effect of the methyl side chain on the permeability properties of polynorbornene-based membranes, were looking for increasing the chain mobility by creating the side-chain within polymer, as well as increase the free volume and decrease the chain stiffness were 63.7 and 5.2 (Barrer), respectively, which are comparable with those of reported previously (Table 3). Additionally, the obtained selectivity was 12.2.

In fact, although obtained results of the permeability were lower than those of polynorbornene membranes having side groups [12], they revealed better results compared to many of the other studies performed on the polynorbornene.

Finally, the combination of the stability of chemical properties and permeability over time, as well as the acceptable permeability and selectivity in the class of glass polymers, making further research on this family of polyolefins can be attractive. Furthermore, there is a need for more attention to research and address the shortcomings of these polymers.

**Table 3** Single Gas Permeability/Selectivity at 30 $^0$C and 1 atm

| Type of Polynorbornene | Permeability (Barrer[a]) | | | | $CO_2/CH_4$ Selectivity | Reference |
|---|---|---|---|---|---|---|
| | $CO_2$ | $CH_4$ | $N_2$ | $O_2$ | | |
| APN-Ni(II) | 63.7 | 5.2 | 3.5 | $O_2$ | 12.2 | This work |
| Romp PN | 15.4 | 2.5 | 1.5 | 16.3 | 6.16 | [4] |
| APN- (R:-$CH_3$) | 396.3 | 30.3 | 24.1 | 2.8 | 13 | [4] |
| APN- Ni($C_6F_5$)$_2$(SbPh$_3$)$_2$ | 28.2 | 2 | 1.9 | 89.2 | 14.1 | [37] |
| APN- Ni[(Nph)$_2$Ni]-methyla-luminoxane | 33.6 | 2.6 | 1.5 | - | 12.9 | [25] |
| APN-Ni(R:-$CH_3$) | 81.1 | 5.6 | 4.3 | 6.9 | 14.5 | [23] |
| APN-Ni(acac)$_2$ | 49.1 | - | 2.7 | - | - | [11] |
| APN-Ni($C_6F_5$)$_2$ | 52 | 3.1 | 2.5 | 10.8 | 16.7 | [21] |
| ROMP-PNB(Catalyst Re) | 23.6 | 4.7 | 2.2 | 11 | 5 | [26] |

[a] 1 Barrer = $10^{-10}$ cm$^3$ (STP) cm/cm$^2$ s cmHg

**Table 4** The HOMO, LUMO energies (eV), and $\Delta E_{L-H}$ as the energy gap ($E_{LUMO} - E_{HOMO}$)

| Molecule | $E_H$ | $E_L$ | $\Delta E_{L-H}$ | $\eta$ |
|----------|-------|-------|------------------|--------|
| $C_7H_{12}$ | -6.64 | 1.41 | 8.05 | -4.025 |
| $CH_4$ | -9.27 | 2.82 | 12.09 | -6.045 |
| $O_2$ | -5.81 | 3.83 | 9.64 | -4.82 |
| $N_2$ | -9.96 | -1.72 | 8.24 | -4.12 |
| $CO_2$ | -8.95 | -0.43 | 8.52 | -4.26 |

**Table 5** The HOMO, LUMO energies (eV), $\Delta E_{L-H}$ as the energy gap ($E_{LUMO} - E_{HOMO}$), $\eta = 1/2$ ($\Delta E_{L-H}$) and the value of optimized energy of relevant clusters

| Cluster | $E_H$ | $E_L$ | $\Delta E_{L-H}$ | $\eta$ | $E_{optm}$ |
|---------|-------|-------|------------------|--------|------------|
| $C_7H_{12}/CH_4$ | -6.59 | 1.29 | 7.88 | 3.94 | -103.5 |
| $C_7H_{12}/O_2$ | -5.73 | -5.72 | 0.01 | 0.005 | -91.4 |
| $C_7H_{12}/N_2$ | -6.66 | -1.78 | 4.88 | 2.44 | -95.7 |
| $C_7H_{12}/CO_2$ | -6.68 | -0.43 | 6.68 | 3.34 | -104.1 |

## Simulation results

The electronic properties of isolated molecules after optimization process are listed in Table 4. Overall, $E_{HOMO}$ shows the capability of a molecule to donate electrons [41], while $E_{LUMO}$ is a criteria regarding the ability of the molecule to receive electrons from other surface. As seen, the $O_2$ and $N_2$ had the highest and lowest HOMO energies, indicating the $O_2$ had the most favorable tendency to donate electron and $N_2$ showed the weakest trend.

Moreover, the highest value of the energy gap $\Delta E_{L-H}$ at 12.9 is ascribed to the $CH_4$, suggesting its more stability compared with other structure. By contrast, $C_7H_{12}$ experienced the lowest $\Delta E_{L-H}$ at 8.05, revealing its high reactivity, compared other molecules. As a result, a low value of the energy gap is a signature of a high reactivity for defines molecule, whereas high stability of the molecule is originated from high value in energy gap. Maroon and his coworkers have been shown similar results in polynorbornene derivatives for $CO_2/N_2$ separation [42].

The calculated adsorption energies of defined clusters after geometry optimization process values are illustrated in Fig. 5.
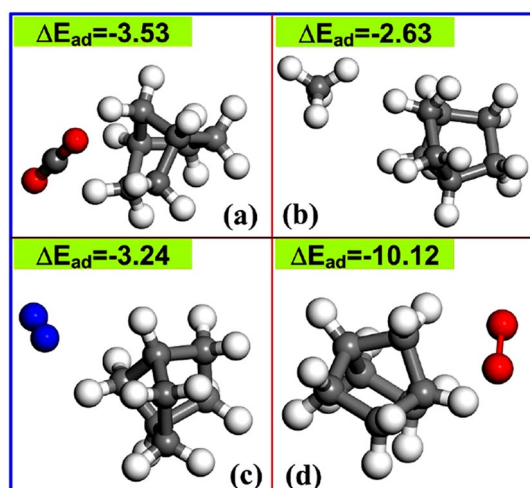


**Fig. 5** The final optimized geometries of **a** $C_7H_{12}/CO_2$, **b** $C_7H_{12}/CH_4$, **c** $C_7H_{12}/N_2$, **d** $C_7H_{12}/N_2$ along with computed energy values

The negative value of the adsorption energy for all clusters confirms the spontaneous adsorption process. In this case, the highest adsorption energy value was determined for $C_7H_{12}/O_2$ cluster, indicating it is the most stable cluster. In other words, $O_2$ molecules have more tendencies to $C_7H_{12}$ than that of other gas molecules and better capability to adsorb onto $C_7H_{12}$. It can be attributed to the formation of stronger (shorter) intermolecular interaction between $C_7H_{12}$ and $O_2$ compared to other complexes.

The electronic properties of optimized clusters at electronic scale, shown in Fig. 5, are summarized in Table 5.

According to the Table 5, it is evident that structures of $C_7H_{12}/CH_4$ and $C_7H_{12}/O_2$ had the highest and lowest $\Delta E_{L-H}$, at 7.88, and 0.01 eV, respectively. It confirms that the $C_7H_{12}/O_2$ cluster saw the highest reactivity and stability compared to other samples. Nevertheless, the outcomes of optimized energy for each complex showed that the $C_7H_{12}/CO_2$ had the highest value, indicating the high stability of this cluster without considering the energy values of isolated molecules. The value of $E_L$ for $C_7H_{12}/CO_2$ was -0.43 eV that is exactly the same as isolated $CO_2$. It reveals that the electron acceptance capability of this cluster is originated from $CO_2$ molecules. The simulation results are in a fair agreement with experimental data. However, there is a little discrepancy between diffusivity data and adsorption energy obtained via DFT simulation. This can be ascribed to the consideration of only the monomer unit of polynorbornene that may restrict the calculation of appropriate chemical interactions (intra and inter molecular) involving between polymer and gas molecules.

## Conclusion

In this research, a dual-core catalyst based on nickel associated with a methylaluminoxane was applied to improve the physical–mechanical properties, film-ability of polynorbornene homopolymer as well as final application in gas separation. The synthesized polynorbornene using this dual-core catalyst had higher molecular weight (902 kg/mol) and a narrow molecular weight distribution (1.9) compared to similar studies reported by others. Furthermore,

such a molecular weight can be soluble in chlorobenzene (trichlorobenzene) solvent family; hence the chance of membrane preparation by casting method was improved. The appearance of two diffraction peaks at XRD pattern of polynorbornene at 2θ: 10 and 20° confirmed its similar crystalline behavior compared to previously synthesized polynorbornene. A dense and porous microstructure is evident based on FESEM micrographs. It was due to the type of solvent used in the polymer film forming process. The permeability values against $CO_2$ and CH4 were 63.7 and 5.2 (Barrer), respectively, which are comparable with those of reported previously. Additionally, the obtained selectivity was 12.2.

DFT-D simulation results showed that $O_2$ molecules have more tendencies to $C_7H_{12}$ than that of other gas molecules and better capability to adsorb onto $C_7H_{12}$.

In fact, obtained results of the permeability were lower than those of polynorbornene membranes having side groups; they revealed better results compared to many of the other studies performed on the polynorbornene. This can open new windows for researchers to design and synthesis polynorbornene with tunable microstructure and consequently excellent gas separation applications.

## Declarations

## References

1. Mol JC (2004) Industrial applications of olefin metathesis. J Mol Catal A Chem 213(1):39–45. https://doi.org/10.1016/j.molcata.2003.10.049
2. Osokin YG (2007) Vinylnorbornene: Preparation, chemical transformations, and use in organic synthesis and polymer chemistry. Vinylnorbornene synthesis and isomerization to ethylidenenorbornene (review). Pet Chem 47:3–14. https://doi.org/10.1134/S096554410701001X
3. Poulsen L, Zebger I, Klinger M et al (2003) Oxygen diffusion in copolymers of ethylene and norbornene. Macromolecules 36:7189–7198. https://doi.org/10.1021/ma034744j
4. Dorkenoo KD, Pfromm PH, Rezac ME (1998) Gas transport properties of a series of high Tg polynorbornenes with aliphatic pendant groups. J Polym Sci Part B Polym Phys 36:797–803. https://doi.org/10.1002/(SICI)1099-0488(19980415)36:5%3c797::AID-POLB7%3e3.0.CO;2-I
5. Yampolskii Y (2010) Norbornene Polymers as Materials for Membrane Gas Separation. Compr Membr Sci Eng 1:131–146. https://doi.org/10.1016/B978-0-08-093250-7.00050-5
6. Bermeshev MV, Chapala PP (2018) Addition polymerization of functionalized norbornenes as a powerful tool for assembling molecular moieties of new polymers with versatile properties. Prog Polym Sci 84:1–46. https://doi.org/10.1016/j.progpolymsci.2018.06.003
7. Alentiev DA, Dzhaparidze DM, Gavrilova NN et al (2018) Microporous materials based on norbornadiene-based cross-linked polymers. Polymers (Basel). https://doi.org/10.3390/polym10121382
8. Finkelshtein ES, Bermeshev MV, Gringolts ML et al (2011) Substituted polynorbornenes as promising materials for gas separation membranes. Russ Chem Rev 80:341–361. https://doi.org/10.1070/rc2011v080n04abeh004203
9. Finkelshtein ES, Gringolts ML, Ushakov NV et al (2003) Synthesis and gas permeation properties of new ROMP polymers from silyl substituted norbornadienes and norbornenes. Polymer (Guildf) 44:2843–2851. https://doi.org/10.1016/S0032-3861(03)00164-2
10. Mansouri S, Omidvar M, Mortazavi SMM et al (2022) 5-Ethylidene-2-norbornene Polymerization by α-Diimine Nickel Catalyst: A revealing insight into the pivotal function of binuclear and mononuclear catalyst structure in tailoring polymer architecture. Macromol Reac Eng 16(2):2100052. https://doi.org/10.1002/mren.202100052
11. Zhao CT, Ribeiro MDR, Portela MF et al (2001) Homo- and copolymerization of norbornene and styrene with nickel bis(acetyl acetonate)/methylaluminoxane system. Eur Polym J 37:45–54. https://doi.org/10.1016/S0014-3057(00)00078-1
12. Finkelshtein ES, Makovetskii KL, Gringolts ML et al (2006) Addition-type polynorbornenes with Si(CH3)3 side groups: Synthesis, gas permeability, and free volume. Macromolecules 39:7022–7029. https://doi.org/10.1021/ma061215h
13. Wozniak AI, Bermesheva EV, Borisov IL et al (2019) Addition polyalkylnorbornenes: A promising new class of si-free membrane materials for hydrocarbons separation. Macromol Rapid Commun 40:1–5. https://doi.org/10.1002/marc.201900206
14. Karpov GO, Alentiev DA, Wozniak AI et al (2020) Dielectric properties of addition and metathesis polynorbornenes with bulky side-substituents. Polymer (Guildf) 203:122759. https://doi.org/10.1016/j.polymer.2020.122759
15. Yampolskii Y (2012) Polymeric gas separation membranes. Macromolecules 45:3298–3311. https://doi.org/10.1021/ma300213b
16. Shakeri SE, Ghaffarian SR, Tohidian M et al (2013) Polyelectrolyte Nanocomposite Membranes, Based on Chitosan-phosphotungstic Acid Complex and Montmorillonite for Fuel Cells Applications. J Macromol Sci Part B 52:1226–1241. https://doi.org/10.1080/00222348.2013.763565
17. Sabzekar M, Pourafshari Chenar M, Maghsoud Z et al (2021) Cyclic olefin polymer as a novel membrane material for membrane distillation applications. J Memb Sci 621:118845. https://doi.org/10.1016/j.memsci.2020.118845
18. Belov N, Nikiforov R, Starannikova L et al (2017) A detailed investigation into the gas permeation properties of addition-type poly(5-triethoxysilyl-2-norbornene). Eur Polym J 93:602–611. https://doi.org/10.1016/j.eurpolymj.2017.06.030
19. Gmernicki KR, Hong E, Maroon CR et al (2016) Accessing Siloxane Functionalized Polynorbornenes via Vinyl-Addition Polymerization for CO2 Separation Membranes. ACS Macro Lett 5:879–883. https://doi.org/10.1021/acsmacrolett.6b00435
20. Wozniak AI, Bermesheva EV, Andreyanov FA et al (2020) Modifications of addition poly(5-vinyl-2-norbornene) and gas-transport properties of the obtained polymers. React Funct Polym 149:104513. https://doi.org/10.1016/j.reactfunctpolym.2020.104513
21. Wilks BR, Chung WJ, Ludovice PJ et al (2003) Impact of average free-volume element size on transport in stereoisomers of polynorbornene. I. Properties at 35 °C. J Polym Sci Part B Polym Phys 41(18):2185–2199. https://doi.org/10.1002/polb.10576
22. Alentiev DA, Egorova ES, Bermeshev MV et al (2018) Janus tricyclononene polymers bearing tri(: N -alkoxy)silyl side groups for membrane gas separation. J Mater Chem A 6:19393–19408. https://doi.org/10.1039/c8ta06034g

23. Karpov GO, Borisov IL, Volkov AV et al (2020) Synthesis and gas transport properties of addition polynorbornene with perfluorophenyl side groups. Polymers (Basel). https://doi.org/10.3390/POLYM12061282

24. Sundell BJ, Lawrence JA, Harrigan DJ et al (2016) Alkoxysilyl functionalized polynorbornenes with enhanced selectivity for heavy hydrocarbon separations. RSC Adv 6:51619–51628. https://doi.org/10.1039/c6ra10383a

25. Finkelshtein ES, Makovetskii KL, Gringolts ML et al (2006) Addition polymerization of silyl-containing norbornenes in the presence of Ni-based catalysts. J Mol Catal A Chem 257:9–13. https://doi.org/10.1016/j.molcata.2006.04.035

26. Peng D, Chen C (2021) Photoresponsive Palladium and Nickel Catalysts for Ethylene Polymerization and Copolymerization. Angew Chemie - Int Ed 60:22195–22200. https://doi.org/10.1002/anie.202107883

27. Wang W, Chen M, Pang W et al (2021) Palladium-Catalyzed Synthesis of Norbornene-Based Polar-Functionalized Polyolefin Elastomers. Macromolecules 54:3197–3203. https://doi.org/10.1021/acs.macromol.1c00201

28. Xu M, Chen C (2021) A disubstituted-norbornene-based comonomer strategy to address polar monomer problem. Sci Bull 66:1429–1436. https://doi.org/10.1016/j.scib.2021.03.012

29. Steinhäusler T, Koros WJ (1997) Gas permeation and sorption studies on stereoregular polynorbornene. J Polym Sci Part B Polym Phys 35:91–99. https://doi.org/10.1002/(SICI)1099-0488(19970115)35:1%3c91::AID-POLB7%3e3.0.CO;2-Y

30. Farquhar AH, Brookhart M, Miller AJM (2020) Oligomerization and polymerization of 5-ethylidene-2-norbornene by cationic palladium and nickel catalysts. Polym Chem 11:2576–2584. https://doi.org/10.1039/d0py00216j

31. Malgas-Enus R, Mapolie SF, Smith GS (2008) Norbornene polymerization using multinuclear nickel catalysts based on a polypropyleneimine dendrimer scaffold. J Organomet Chem 693:2279–2286. https://doi.org/10.1016/j.jorganchem.2008.03.029

32. Rong C, Li W, Tan C (2019) Monodentate aminophosphine nickel(II)- and palladium(II)-catalyzed ethylene oligomerization and norbornene polymerization. Appl Organomet Chem 33:1–8. https://doi.org/10.1002/aoc.4631

33. Liu H, Yuan H, Shi X (2019) Synthesis of nickel and palladium complexes with diarylamido-based unsymmetrical pincer ligands and application for norbornene polymerization. Dalt Trans 48:609–617. https://doi.org/10.1039/c8dt04413a

34. Khoshsefat M, Dechal A, Ahmadjo S et al (2018) Synthesis of poly(α-olefins) containing rare short-chain branches by dinuclear Ni-based catalysts. New J Chem 42:18288–18296. https://doi.org/10.1039/c8nj04481c

35. Dechal A, Khoshsefat M, Ahmadjo S et al (2018) Mono- and binuclear nickel catalysts for 1-hexene polymerization. Appl Organomet Chem 32:1–9. https://doi.org/10.1002/aoc.4355

36. Khoshsefat M, Dechal A, Ahmadjo S et al (2019) Cooperative effect through different bridges in nickel catalysts for polymerization of ethylene. Appl Organomet Chem 33:1–12. https://doi.org/10.1002/aoc.4929

37. Shakeri SE, Mortazavi SMM, Ahmadjo S, Zohuri GH (2020) Comparison of mono and dinuclear α–diimine Ni-based catalysts for synthesis of polynorbornene and its microstructure study. J Macromol Sci Part A Pure Appl Chem 57:837–843. https://doi.org/10.1080/10601325.2020.1796494

38. Hosseini H, Mousavi SM (2020) Density functional theory simulation for Cr(VI) removal from wastewater using bacterial cellulose/polyaniline. Int J Biol Macromol 165:883–901. https://doi.org/10.1016/j.ijbiomac.2020.09.217

39. Hosseini H, Mousavi SM, Wurm FR, Goodarzi V (2021) Display of hidden properties of flexible aerogel based on bacterial cellulose/polyaniline nanocomposites with helping of multiscale modeling. Eur Polym J. https://doi.org/10.1016/j.eurpolymj.2020.110251

40. Dujardin W, Van Goethem C, Steele JA et al (2019) Polyvinylnorbornene gas separation membranes. Polymers (Basel). https://doi.org/10.3390/polym11040704

41. Hosseini H, Zirakjou A, McClements DJ et al (2022) Removal of methylene blue from wastewater using ternary nanocomposite aerogel systems: Carboxymethyl cellulose grafted by polyacrylic acid and decorated with graphene oxide. J Hazard Mater 421:126752. https://doi.org/10.1016/j.jhazmat.2021.126752

42. Maroon CR, Townsend J, Higgins MA et al (2020) Addition-type alkoxysilyl-substituted polynorbornenes for post-combustion carbon dioxide separations. J Memb Sci 595:117532. https://doi.org/10.1016/j.memsci.2019.117532